Electronic Supplementary Material (ESI) for Soft Matter.

Electronic Supplementary Information

1. Comparison between neo-Hookean model and Yeoh model

The neo-Hookean material (NH) is a special case of the Yeoh's model with $C_2 = C_3 = 0$. For this case, the normalized nominal stress in a uniaxial test has no softening and hardening behavior (Figure S1) and will not fit the experimental data in Chopin et al.[1] or Deplace et al.[2] Nevertheless, we plot the lateral and shear stresses based on this model and compare with Kaelble's prediction. These results are plotted below. This figure shows that our conclusion that the lateral stress τ_{11} is much larger than the shear stress τ_{12} in the adhesive for a large shear strain γ is still valid.

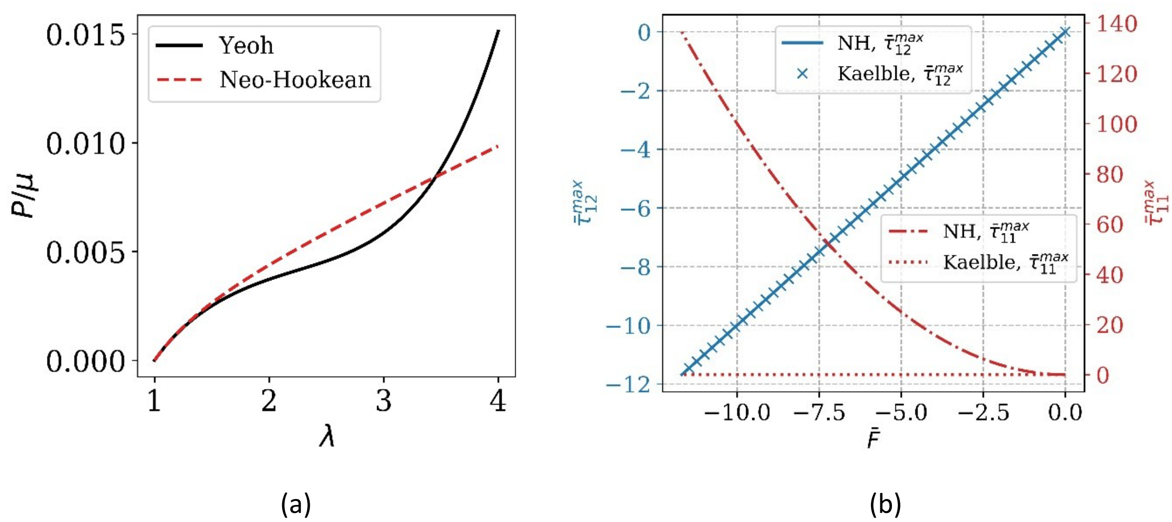

Figure S1. (a) Normalized nominal stress versus stretch for neo-Hookean and Yeoh materials, plotted as dashed and solid lines, respectively. (b) Normalized peel force $\bar{F}$ versus maximum normalized shear $\bar{\tau}_{12}^{\max}$ and lateral normal stress $\bar{\tau}_{11}^{\max}$ based on a neo-Hookean material. The linear theory of Kaelble is plotted in this same figure for comparison. Note linear theory of Kaelble assumes $\tau_{11} = 0$.

2. Derivation of equation (16)

The key to solving (5) is to make γ the independent variable and $\eta = x / l_{LT}$ the dependent variable, thus

$$\frac{d}{d\eta} = \frac{d\gamma}{d\eta}\frac{d}{d\gamma} \Rightarrow \frac{d}{d\eta}\left(\frac{d\gamma}{d\eta}\right) = \frac{d\gamma}{d\eta}\frac{d}{d\gamma}\left(\frac{1}{d\eta / d\gamma}\right) = \left(\frac{-1}{\left(d\eta / d\gamma\right)^3}\right)\frac{d^2\eta}{d\gamma^2} \tag{S1}$$

Using (S1), (5) becomes:

$$\frac{d^2\eta}{d\gamma^2} = -\left(d\eta / d\gamma\right)^{-3}\hat{\tau}(\gamma) \tag{S2}$$

where $\hat{\tau} \equiv \tau / \mu = f(\gamma)\gamma$. Next, let $\varphi = d\eta / d\gamma$, then (S2) turns into a first order separable equation:

$$\frac{d\varphi}{d\gamma}=-\varphi^3 f(\gamma)\gamma \Rightarrow \frac{1}{\varphi^2}=\frac{1}{\varphi^2}=2\int_0^{\gamma}\gamma' f(\gamma')d\gamma' \Rightarrow \frac{d\eta}{d\gamma}=\left[2\int_0^{\gamma}\gamma' f(\gamma')d\gamma'\right]^{-1/2} \tag{S3}$$

where the integration constant is determined by the condition $\gamma=0$ at $\eta=\infty$. Note that in our coordinate system, γ is negative, so the integral in the RHS of (S3) is positive. We expect $d\gamma/d\eta>0$, so we pick the positive square root in (S3). We integrate (S3) to give:

$$\eta=-\int_{\gamma_0}^{\gamma}\left[2\int_0^{w} f(\gamma')\gamma' d\gamma'\right]^{-1/2} dw \tag{S4}$$

where the integration constant is determined by the condition $\gamma(\eta=0)=\gamma_0$, where γ_0 is the as yet unknown maximum shear strain at the origin. The solution can be obtained using any smooth $f(\gamma)$. Here we consider the special case where the material model is given by the three-term Yeoh's model:

$$f(\gamma)=\left(1+\frac{4C_2}{\mu}\gamma^2+\frac{6C_3}{\mu}\gamma^4\right) \tag{S5}$$

For this case, (S4) can be evaluated exactly and is:

$$\eta=\int_{-\gamma}^{-\gamma_0}\frac{dw}{w\sqrt{1+\frac{4C_2}{\mu}w^2+\frac{6C_3}{\mu}w^4}}=\ln\left|\frac{\gamma_0}{\gamma}\right|-\frac{1}{2}\ln\left[\frac{\sqrt{1+\frac{2C_2}{\mu}\gamma_0^2+\frac{2C_3}{\mu}\gamma_0^4}+\frac{C_2}{\mu}\gamma_0^2+1}{\sqrt{1+\frac{2C_2}{\mu}\gamma^2+\frac{2C_3}{\mu}\gamma^4}+\frac{C_2}{\mu}\gamma^2+1}\right] \tag{S6}$$

To invert (16a), we note

$$\begin{aligned}\eta&=\ln\left|\frac{\gamma_0}{\gamma}\right|-\frac{1}{2}\ln\left[\frac{\gamma_0^2\left(\sqrt{\gamma_0^{-4}+\frac{2C_2}{\mu}\gamma_0^{-2}+\frac{2C_3}{\mu}}+\frac{C_2}{\mu}+\gamma_0^{-2}\right)}{\gamma^2\left(\sqrt{\gamma^{-4}+\frac{2C_2}{\mu}\gamma^{-2}+\frac{2C_3}{\mu}}+\frac{C_2}{\mu}+\gamma^{-2}\right)}\right]\\&=-\frac{1}{2}\ln\left[\frac{\sqrt{\gamma_0^{-4}+\frac{2C_2}{\mu}\gamma_0^{-2}+\frac{2C_3}{\mu}}+\frac{C_2}{\mu}+\gamma_0^{-2}}{\sqrt{\gamma^{-4}+\frac{2C_2}{\mu}\gamma^{-2}+\frac{2C_3}{\mu}}+\frac{C_2}{\mu}+\gamma^{-2}}\right]\end{aligned} \tag{S7}$$

If we denote $A(\gamma_0)\equiv\sqrt{\gamma_0^{-4}+\frac{2C_2}{\mu}\gamma_0^{-2}+\frac{2C_3}{\mu}}+\frac{C_2}{\mu}+\gamma_0^{-2}$ and $y=\gamma^{-2}$, (S7) is:

$$e^{-2\eta}=\frac{A(\gamma_0)}{\sqrt{y^2+\frac{2C_2}{\mu}y+\frac{2C_3}{\mu}}+\frac{C_2}{\mu}+y}\Rightarrow\sqrt{y^2+\frac{2C_2}{\mu}y+\frac{2C_3}{\mu}}=A(\gamma_0)e^{2\eta}-\left(\frac{C_2}{\mu}+y\right) \tag{S8}$$

Squaring both sides of (S8), we have

$$2A(\gamma_0)e^{2\eta}y = A^2(\gamma_0)e^{4\eta} - 2A(\gamma_0)e^{2\eta}\left(\frac{C_2}{\mu}\right) + \left(\frac{C_2}{\mu}\right)^2 - \frac{2C_3}{\mu}$$
$$\Rightarrow y = \frac{1}{\gamma_0^2} = \frac{A(\gamma_0)e^{2\eta}}{2} - \frac{C_2}{\mu} + \frac{e^{-2\eta}}{2A(\gamma_0)}\left[\left(\frac{C_2}{\mu}\right)^2 - \frac{2C_3}{\mu}\right] \tag{S9}$$

3. Calculation of peel force (17)

$$F/b = \mu l_{LT}\int_0^\infty f(\gamma)\gamma d\eta = -\mu l_{LT}\int_0^{\gamma_0} f(\gamma)\gamma\frac{d\eta}{d\gamma}d\gamma = -\frac{\mu l_{LT}}{\sqrt{2}}\int_0^{\gamma_0} f(\gamma)\gamma\left[\int_0^{\gamma}\gamma' f(\gamma')d\gamma'\right]^{-1/2}d\gamma \tag{S10}$$

Next, let $\chi = \int_0^{\gamma}\gamma' f(\gamma')d\gamma'$, then $d\chi/d\gamma = \gamma f(\gamma)$, then S7 is

$$F/b = -\frac{\mu l_{LT}}{\sqrt{2}}\int_0^{\chi_\infty}\chi^{-1/2}d\chi = -\mu l_{LT}\sqrt{2\chi_\infty} \tag{S11a}$$

where

$$\chi_\infty = \int_0^{\gamma_0}\gamma' f(\gamma')d\gamma' \tag{S11b}$$

Equation (S8) does not depend on the specific form of the hyperelastic model, provided that the strain energy density function depends only on I_1. For the three-term Yeoh solid, the peel force is related to the maximum shear strain γ_0 by

$$F/b = -\mu l_{LT}|\gamma_0|\sqrt{1 + \frac{c_2}{2}|\gamma_0|^2 + \frac{c_3}{3}|\gamma_0|^4} \tag{S12}$$

4. Normalized peel force versus maximum shear strain with two different sets of parameters

We use two more sets of material parameters to find the dependence of the normalized peel force on the maximum shear strain: one set has a larger softening term $2C_2$, while the other has a larger hardening term $2C_3$ (the original set in the main text of the paper is $\{C_1, C_2, C_3\}$). As shown in Fig. S2 below, the qualitative behavior remains the same – there is still a substantial difference between linear and nonlinear theory.

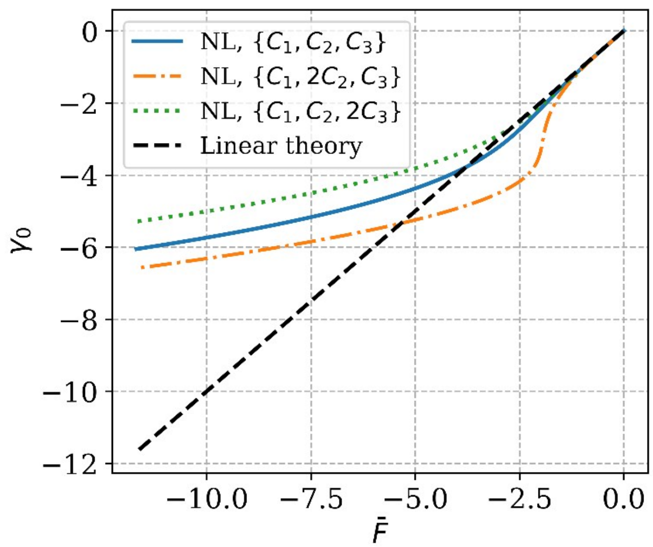

Figure S2. Normalized peel force $\bar{F}$ versus maximum shear strain γ_0 at peel front. Nonlinear theory and linear theory (Kaelble) predictions, for various $\bar{F}$, are plotted as solid and dashed lines respectively. Also, different sets of parameters with softer (dash-dotted line) or stiffer (dotted line) behaviors are also plotted for comparison.

5. Stresses along the adhesive/backing interface

The stress fields along the adhesive/backing interface are plotted in Fig S3. As expected, these stresses are practically the same in region 2 and agree well with our analytic model.

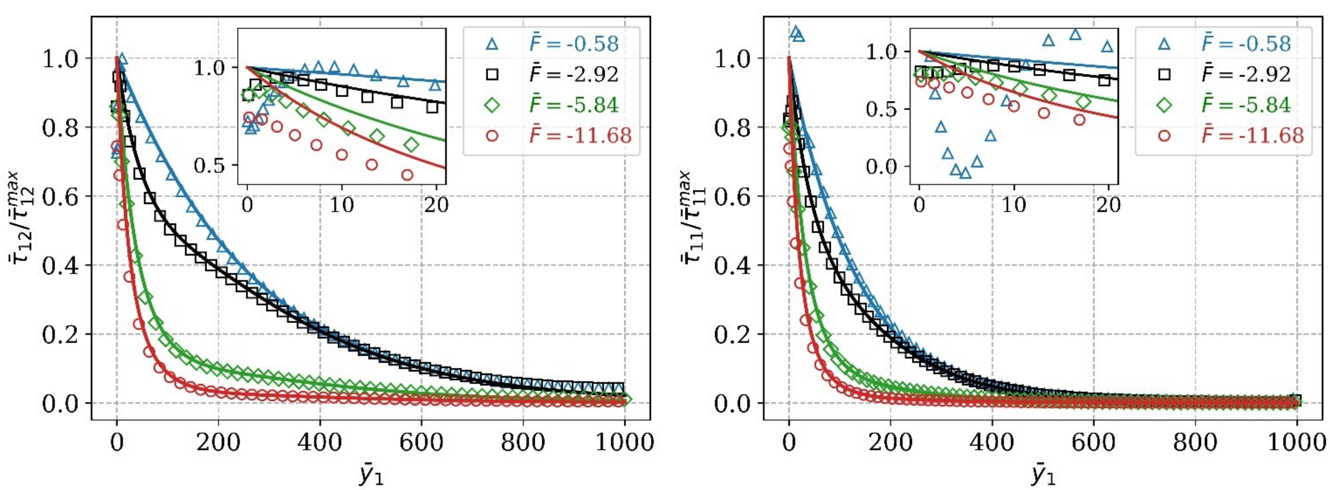

(a)

(b)

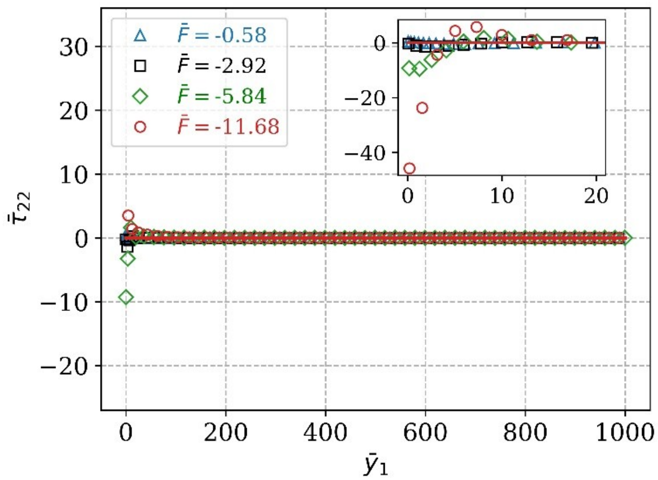

(c)

Fig S3. True stress (normalized) along the adhesive/backing interface with different applied loads. Analytic solutions and FEM results are plotted as solid lines and symbols respectively. The triangular, square, diamond and circle symbols indicate different applied force, i.e., $\bar{F}$ = -0.58, -2.92, -5.84 and -11.68 respectively. The true stresses near the origin are plotted in the insets. (a) $\bar{\tau}_{12} / \bar{\tau}_{12}^{\max}$. (b) $\bar{\tau}_{11} / \bar{\tau}_{11}^{\max}$. (c) $\bar{\tau}_{22}$.

6. Stresses in region 1 with an applied force $\bar{F} = -11.68$

Here we plot $\bar{\tau}_{12}$, $\bar{\tau}_{11}$ and $\bar{p}$ along the adhesive/substrate and adhesive/backing interfaces in region 1 in Fig.S4 and Fig.S5, respectively.

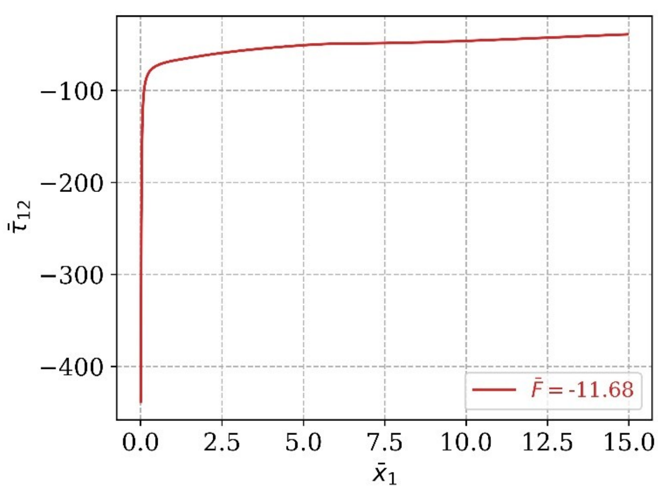

(a)

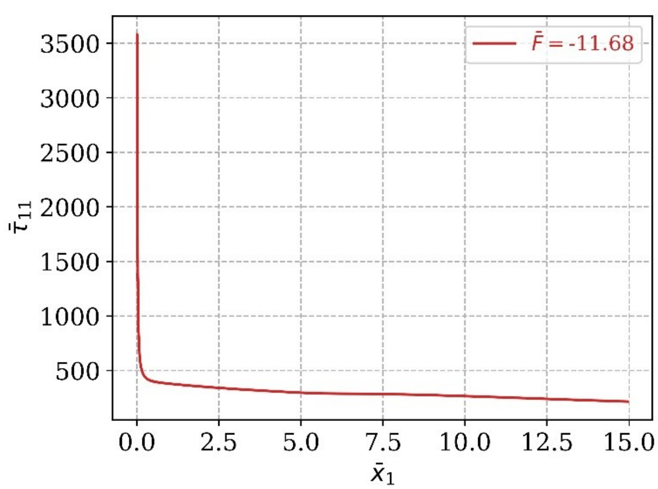

(b)

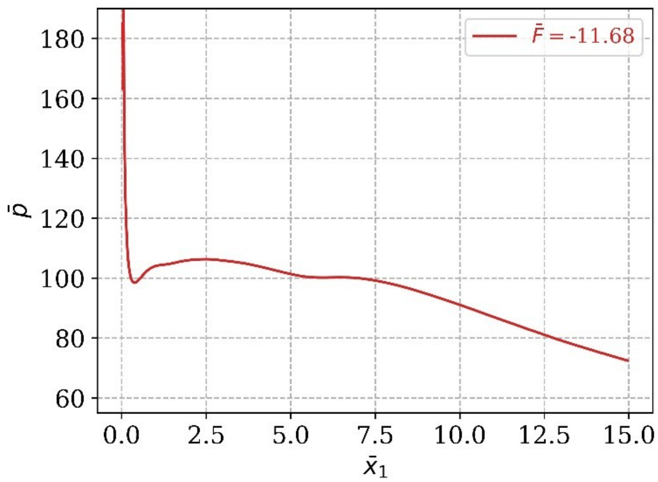

(c)

Fig. S4. True Stress and pressure (normalized) along the adhesive/substrate interface with an applied force $\bar{F} = -11.68$. (a) $\bar{\tau}_{12}$; (b) $\bar{\tau}_{11}$ and (c) $\bar{p}$.

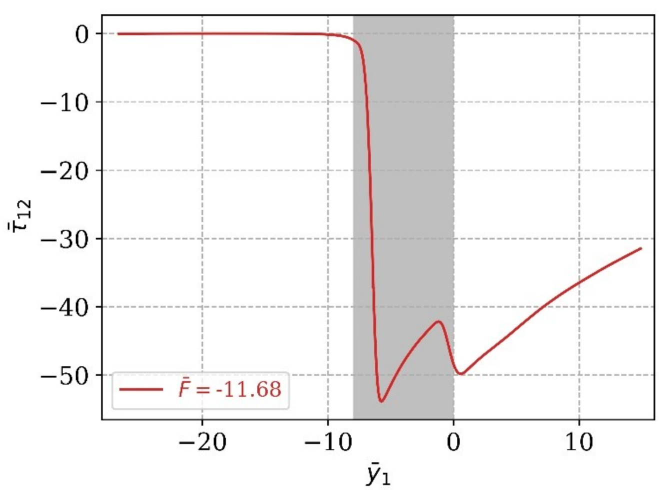

(a)

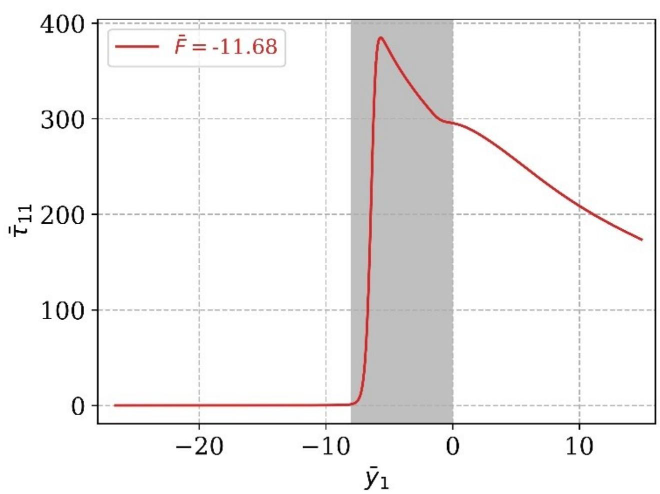

(b)

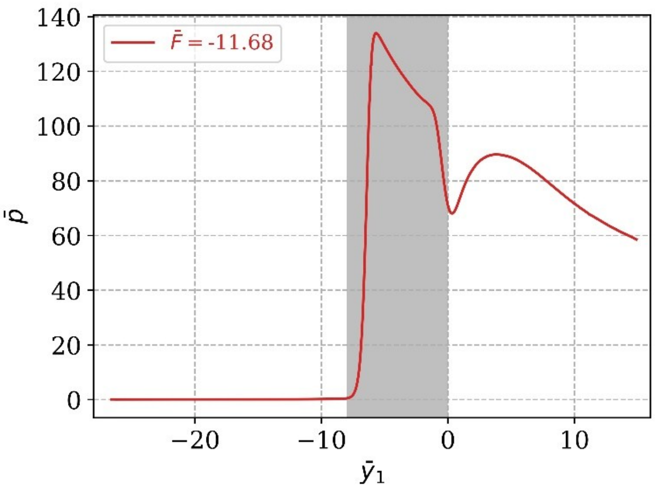

(c)

Fig. S5. True stresses and pressure (normalized) along the adhesive/backing interface with an applied force $\bar{F} = -11.68$. (a) $\bar{\tau}_{12}$; (b) $\bar{\tau}_{11}$ and (c) $\bar{p}$.

7. Effect of viscoelasticity

In the beginning of the test, when the load has just been applied, a linear viscoelastic adhesive will respond to the load like a hyperelastic solid with the short time moduli. For times long compared with the relaxation time of the adhesive, the adhesive will behave like a softer hyper-elastic solid with long time or plateau modulus. This means that our analysis is valid for short and long times.

A difficulty is that there is no universally accepted 3D nonlinear viscoelastic model for adhesive behavior. Here we carried out a preliminary study of viscoelastic effect using a simple linear viscoelastic model: we replace the moduli in the Yeoh model by relaxation moduli with a one-term Prony Series (that means the adhesive has only one relaxation time), that is,

$$C_i(t) = C_i(t=\infty) + C_i(t=\infty)e^{-t/\tau} \quad i = 1,2,3$$

where τ is the characteristic relaxation time. We carried out finite element (FE) simulations using this model. In Figure S6 we plot the FE shear strain γ versus normalized position $\bar{x}_1$.with different time. The applied force in figure S6 is $F/b = -5.84C_1(t=\infty)l_{LT}(t=\infty)$. We also plot our analytic result by simply substituting the relaxation moduli into equations (16-18). As expected, the shear strain distribution along the interface predicted by FEM and our analytic solution is the same for short and long-times. At intermediate times (e.g. t = relaxation time) the shear strain distribution is bounded by these two limits. Surprisingly, our analytical solution agrees well with the finite element result at this intermediate time.

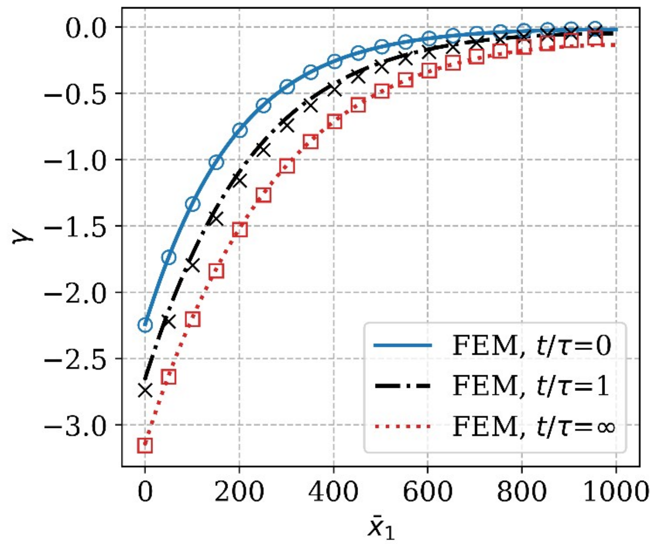

Figure S6. Shear strain γ plotted versus normalized position $\overline{x}_1$ .with different time. FEM results are presented by different lines, and symbols are the analytic solution obtained using eqs.(16-18).

Reference

1 J. Chopin, R. Villey, D. Yarusso, E. Barthel, C. Creton and M. Ciccotti, *accepted in Macromolecules*.

2 F. Deplace, C. Carelli, S. Mariot, H. Retsos, A. Chateauminois, K. Ouzineb and C. Creton, *The Journal of Adhesion*, 2009, **85**, 18–54.